

# Jet velocity in SS 433: its anti-correlation with precession-cone angle and a dependence on orbital phase

Katherine M. Blundell<sup>1</sup> and Michael G. Bowler<sup>1</sup>

## ABSTRACT

We present a re-analysis of the optical spectroscopic data on SS 433 from the last quarter-century and demonstrate that these data alone contain systematic and identifiable deviations from the traditional kinematical model for the jets: variations in jet speed which agree with our analysis of recent radio data, in precession cone angle and in phase. We present a simple technique for separating out the jet speed from the angular properties of the jet axis, assuming only that the jets are symmetric. With this technique, the archival optical data additionally reveal that the variations in jet speed and in precession-cone angle are anti-correlated in the sense that when faster jet bolides are ejected the cone opening angle is smaller. We also find speed oscillations as a function of *orbital* phase.

*Subject headings:* Stars: Binaries: Close, Radio Continuum: Stars, Stars: Individual: SS 433

## 1. Introduction

In a recent paper (Blundell & Bowler 2004), we presented the deepest yet radio image of SS 433 which revealed an historical record over two complete precession periods of the geometry of the jet ejection. Detailed analysis of this image confirmed the approximate values for the standard kinematic model of this object (Margon 1984; Eikenberry et al 2001) but revealed systematic and identifiable deviations from it. Variations in jet speed, lasting for as long as tens of days, were needed to match the detailed structure of each jet. Remarkably, these variations were equal and opposite, matching the two jets simultaneously.

We found the optical data in the literature to be entirely consistent with velocity variations; thus our findings from the radio image led us to re-analyse the archival optical data.

---

<sup>1</sup>University of Oxford, Department of Physics, Keble Road, Oxford, OX1 3RH, U.K.

We are most grateful to George Collins II and Bruce Margon for making available to us electronically their accumulated data sets. In the analysis presented in this paper, we use solely Collins’ dataset (published in Collins & Scher 2000) because of its higher quoted precision, but very similar results are obtained from Margon’s dataset.

## 2. Speed and angular variations from the optical data

If the precessing jet axis of SS 433 traces out a cone of semi-angle  $\theta$  about a line which is oriented at an angle  $i$  to our line-of-sight with jet velocity  $\beta$  in units of  $c$  ( $\gamma = (1 - \beta^2)^{-1/2}$ ), the redshifts measured from the west jet ( $z_+$ ) and the east jet ( $z_-$ ) are given, if the jets are symmetric, by:

$$z_{\pm} = -1 + \gamma[1 \pm \beta \sin \theta \sin i \cos \phi \pm \beta \cos \theta \cos i], \quad (1)$$

where  $\phi$  is the phase of the precession cycle (and the subject of Appendix A).

Addition of the expressions for  $z_+$  and  $z_-$  in Eqn 1 gives an expression relating the observed pair of redshifts to the jet speed independently of any angular variation. Rearrangement of this expression gives:

$$\beta = \left[ 1 - \left[ 1 + \frac{z_+ + z_-}{2} \right]^{-2} \right]^{1/2}, \quad (2)$$

which contains no dependence on any angular properties, if the jets are symmetric. The quantity  $z_+ + z_-$  fluctuates very substantially (see Fig 1).

Conversely, subtraction of the expressions for  $z_+$  and  $z_-$  in Eqn 1 gives an expression relating the observed pair of redshifts to the angular properties  $a$  of the orientation of the jet axis, from which the speed may be divided out using Eqn 2:

$$a = \frac{z_+ - z_-}{2\beta\gamma} = \sin \theta \sin i \cos \phi + \cos \theta \cos i, \quad (3)$$

which contains no dependence on speed, if the jets are symmetric.

## 3. Jet symmetry and the use of redshift pairs

The detailed correspondence in velocity variations required by both radio jets (Blundell & Bowler 2004) are an encouraging indication that the assumption of symmetry is likely to be justified. There the standard deviation on the difference in the speeds of the two jets is less than  $0.004c$  and the standard deviation of the jet velocity is  $0.014c$ .

The merits of the variables  $s = z_+ + z_-$  and  $a$  (Eqn 3) are exemplified by Fourier analyses of the time distribution of these variables, taken from the Collins’ data set. We used the algorithm developed by Roberts et al (1987) which accounts for the uneven time-sampling of the data by deconvolution (exactly analogous to techniques used in aperture synthesis). The angular data  $a$  clearly revealed periodicities corresponding to the well-known nodding of the precession axis (Katz et al 1982; Newsom & Collins 1982; Collins & Scher 2002) and of course the 162-day precession period; these can be clearly seen in Fig 2a. There is no evidence of any periodicity in the speed data  $s$  (Fig 2b) common to periodicity in the angular data. These results are consistent with perfect symmetry. The speed data also indicate a periodicity at 13.08 days (the periodicity at 12.58 days is a beat with Earth’s orbital period 365 days); to investigate the veracity of this, we folded the data over 13.08 days in 20 phase bins, and within these bins the mean speeds ( $\beta$ , from Eqn 2) were derived. Fig 3 shows a clear sinusoidal oscillation as a function of orbital phase. The rms variation in speed which oscillates with orbital phase is smaller by a factor of three than the dispersion in overall speed oscillations. It is possible that the speed with which bolides are ejected is genuinely a function of orbital phase, but the excursions in Fig 3 could also be interpreted as due to orbital motion; in this case the orbital speed would be  $\sim 400 \text{ km s}^{-1}$ .

#### 4. Anti-correlated deviations in jet speed and $\theta$

We fitted Collins’ dataset with the kinematic model, including nodding. From our fit, we derived the model redshifts and the variables  $s$  and  $a$ . Subtraction of these model variables from those constructed from the Collins’ dataset gave residuals in  $s$  ( $\Delta s$ ) and in  $a$  ( $\Delta a$ ). The  $\beta$  variation is shown in Fig 1c. The standard deviation of this histogram is 0.013 in excellent agreement with the result from our recent radio image (0.014). Examples of the residuals in  $s$  and in the angular variable  $a$  are plotted in Fig 1; the variations in speed and angular residuals are anti-correlated. From Eqns 2 and 3, maintaining the assumption of symmetry:

$$\Delta s^2 = 4\beta^2\gamma^6\Delta\beta^2, \quad (4)$$

$$\begin{aligned} \Delta a^2 &= (\cos\theta \sin i \cos\phi - \sin\theta \cos i)^2\Delta\theta^2 + (\sin\theta \sin i \sin\phi)^2\Delta\phi^2 \\ &- 2 \sin\theta \sin i \sin\phi(\cos\theta \sin i \cos\phi - \sin\theta \cos i)\Delta\theta\Delta\phi, \end{aligned} \quad (5)$$

$$\begin{aligned} \Delta a \Delta s &= 2\beta\gamma^3[(\cos\theta \sin i \cos\phi - \sin\theta \cos i)\Delta\beta \Delta\theta \\ &- \sin\theta \sin i \sin\phi\Delta\beta\Delta\phi], \end{aligned} \quad (6)$$

where  $\Delta\beta$ ,  $\Delta\theta$  and  $\Delta\phi$  represent the variations in  $\beta$ ,  $\theta$  and  $\phi$  respectively. The data contain many cycles; averaging over cycles for any given value of the phase  $\phi$  yields the averages

$\langle \Delta a^2 \rangle$ ,  $\langle \Delta s^2 \rangle$ ,  $\langle \Delta a \Delta s \rangle$  as functions of  $\phi$ , in terms of the parameters  $\langle \Delta \beta^2 \rangle$ ,  $\langle \Delta \theta^2 \rangle$ ,  $\langle \Delta \beta \Delta \theta \rangle$  and so on. The fit to  $\langle \Delta \beta \Delta \theta \rangle$  is shown in Fig 4. All fits are tabulated in Table 1.

Fig 4 shows that the quantity  $\langle \Delta a \Delta s \rangle$  has an almost pure cosinusoidal variation with phase, as given by the first term on the right hand side of Eqn 6. This shape is the unique signature of a correlation between variations in  $\beta$  and in  $\theta$ , in this case negative. While Eqns 4–6 apply for complete symmetry, equivalent expressions can be obtained for fluctuations which are not completely symmetric. Even the 25 year data sets which exist do not have the precision to pick out small contributions from asymmetric excursions but the asymmetric analogues of the significant parameters in Table 1 are at least an order of magnitude smaller and could be zero.

$\langle \Delta \beta^2 \rangle$  shows no correlation with phase and  $\langle \Delta a^2 \rangle$  very little. The latter requires fluctuations in both theta and in phase. We remark that  $\langle \Delta(z_+ - z_-) \Delta s \rangle$  does not show a strong correlation with phase; nor should it, using the parameters from Table 1. Removing the varying speed from  $z_+ - z_-$  was crucial in revealing this correlation in  $\langle \Delta a \Delta s \rangle$ .

## 5. The redshift residual plot

It is instructive to consider the influence on the plane of redshift residuals (as shown e.g. in figure 5 of Eikenberry et al (2001)) of excursions from the kinematic model in  $\beta$ ,  $\theta$  and  $\phi$  or a combination of these. Comparison of their figure 5 (which is very similar to our Fig 5f) with our Figs 5a and 5b mandates the presence of both angular variations (to spread the distribution of points along the line  $y = -x$ ) and velocity variations (to spread the distribution of points perpendicular to this line — note that even their quoted redshift measurement error of 0.003, likely to be an over-estimate in general, is insufficient to account for this breadth).

Inclusion of all these variations, correlated in the way we found in § 4, gives a distribution (Fig 5d) which resembles that from the real data (Fig 5f). The simulations presented in Fig 5d take no account of the (stochastic) duration of the excursions; the deviations shown arise from deviations randomly drawn for each “observation”. Some of the small-scale clumping in the distribution of points seen in Fig 5f but not in Fig 5d appears when account is taken of the variations seen in speed having a timescale of a few days. The duration of variations in Fig 5e were randomly drawn from a gaussian distribution with a half-width of two days.

## 6. Concluding remarks

Investigation of archival optical spectroscopic data on SS 433 reveals variations in jet speed, in cone opening angle, and in the phase of the precession, relative to the standard kinematic model and after accounting for nodding. These are revealed in the plane of redshift residuals (Fig 5) or by the new technique of combining simultaneously observed redshift pairs which give forms for the speed-only ( $s$ ) and angular-only ( $a$ ) characteristics (Fig 1). The first gives the excursions in  $\beta$  (Fig 1); the second gives rms excursions in  $\Delta\theta$ ,  $\Delta\phi$  and the cross-correlations (Table 1 and Fig 4). Variations in jet speed and in cone angle are strongly anti-correlated (correlation coefficient  $-0.7$ ), in the sense that when faster bolides are ejected the cone angle is smaller. We also found smaller amplitude sinusoidal oscillations in speed as a function of orbital phase. If this is due to variations of ejection speed, perhaps the orbit of the binary is eccentric. If these 13.08-day oscillations are orbital Doppler shifts the orbital velocity is  $\sim 400\text{km s}^{-1}$ . If this were the case, the mass of the companion to SS 433 would be  $> 86 M_{\odot}$  and for a mass ratio of  $0.1 \sim 100 M_{\odot}$ . Such masses would be hardly consistent with an A-type companion (Gies et al 2002; Charles et al 2004).

K.M.B. thanks the Royal Society for a University Research Fellowship. We are very grateful to George Collins II for an electronic version of his published data set and to Steven Eikenberry for the electronic version of the Margon data set used in Eikenberry et al (2001). It is a pleasure to thank Avinash Deshpande, James Binney & Philipp Podsiadlowski for helpful discussions.

## REFERENCES

- Anderson, S.F., Margon, B., & Grandi, S.A. 1983, ApJ, 273, 697
- Blundell, K.M. & Bowler, M.G., 2004, ApJ Letters in press
- Charles, P.A. et al, 2004, RevMexAA, 20, 50
- Crampton, D. & Hutchings, J.B. 1981, ApJ, 251, 604
- Collins, G.W. & Scher, R.W., 2002, MNRAS, 336, 1011
- Collins, G.W. & Scher, R.W., 2000, in “the Kth Reunion”, ed A.G.D. Philip, L. Davis Press, Schenectady, NY, pg105
- Eikenberry, S.S., Cameron, P.B., Fierce, B.W., Kull, D.M., Dror, D.H., Houck, J.R., & Margon, B. 2001, ApJ, 561, 1027

- Gies, D.R., Huang, W. & McSwain, M.V., 2002, *ApJ*, 578, L67
- Katz, J. I., Anderson, S. F., Grandi, S. A., & Margon, B. 1982, *ApJ*, 260, 780
- Kemp, J.C., et al. 1986, *ApJ*, 305, 805
- Liebert, J., Angel, J.R.P., Hege, E.K., Martin, P.G., & Blair, W.P. 1979, *Nature*, 279, 384
- Margon, B. 1984, *ARA&A*, 22, 507
- Margon, B., Ford, H.C., Grandi, S.A., & Stone, R.P.S., 1979b, *ApJ*, 233, L63
- Margon, B. & Anderson, S.F. 1989, *ApJ*, 347, 448
- Newsom, G.H. & Collins, G.W., 1982, *ApJ*, 262, 714
- Roberts, D.H., Lehar, J. & Dreher, J.W., 1987, *AJ*, 93, 968
- Stirling, A.M., Jowett, F.H., Spencer, R.E., Paragi, Z., Ogle, R.N., & Cawthorne, T.V.  
2002, *MNRAS*, 337, 657
- Vermeulen, R.C., 1989, PhD thesis, University of Leiden

Table 1. Fits to excursions from the standard kinematic model (incorporating nodding) of SS 433.  $\beta$  is in units of  $c$ , and  $\theta$  and  $\phi$  are in units of radians.

Quantity	fitted value	quantity	derived value
$\langle \Delta\beta^2 \rangle$	$1.67 \pm 0.18 \times 10^{-4}$	rms speed variation	$0.0129c$
$\langle \Delta\theta^2 \rangle$	$2.24 \pm 0.35 \times 10^{-3}$	rms $\theta$ variation	2.71 deg
$\langle \Delta\phi^2 \rangle$	$1.31 \pm 0.26 \times 10^{-2}$	rms $\phi$ variation	2.96 days
$\langle \Delta\beta\Delta\theta \rangle$	$-3.81 \pm 0.52 \times 10^{-4}$		
$\langle \Delta\beta\Delta\phi \rangle$	$1.70 \pm 0.80 \times 10^{-4}$		
$\langle \Delta\theta\Delta\phi \rangle$	indistinguishable from zero		

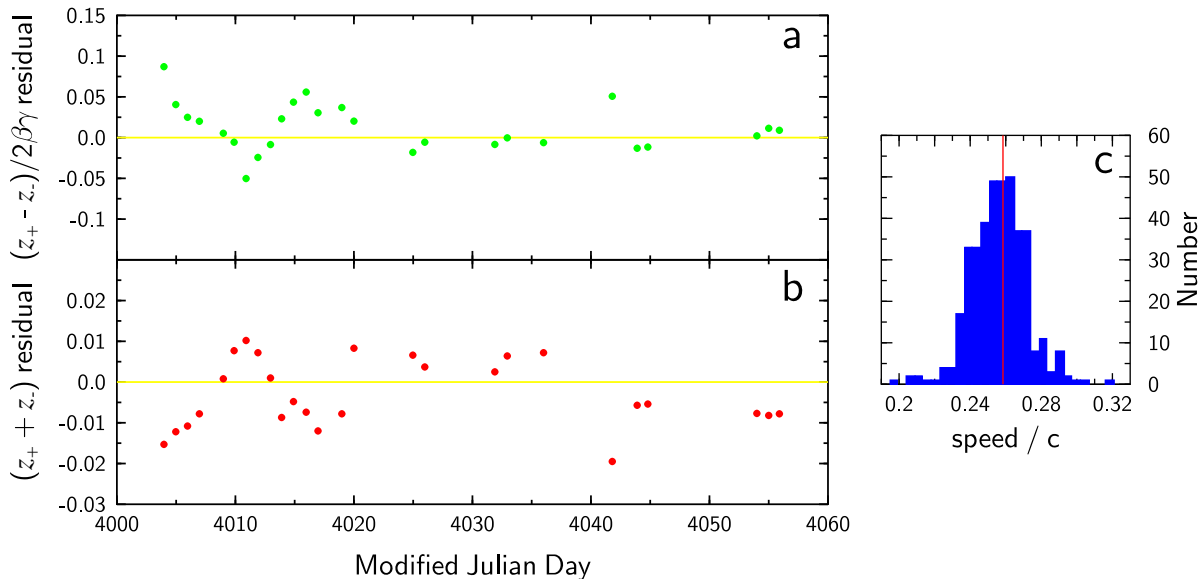


Fig. 1.— **(a)** and **(b)** examples of angular and speed residuals versus time. The variations are suggestive of anti-correlation, which we investigate in §4. **(c)** Distribution of speeds from the data accumulated by Collins over 20 years. The mean is indicated by the vertical red line, and the standard deviation in  $\beta$  is 0.013. The distribution of speeds inferred from effectively one year’s worth of data from the radio image of Blundell & Bowler (2004), has a standard deviation of 0.014.

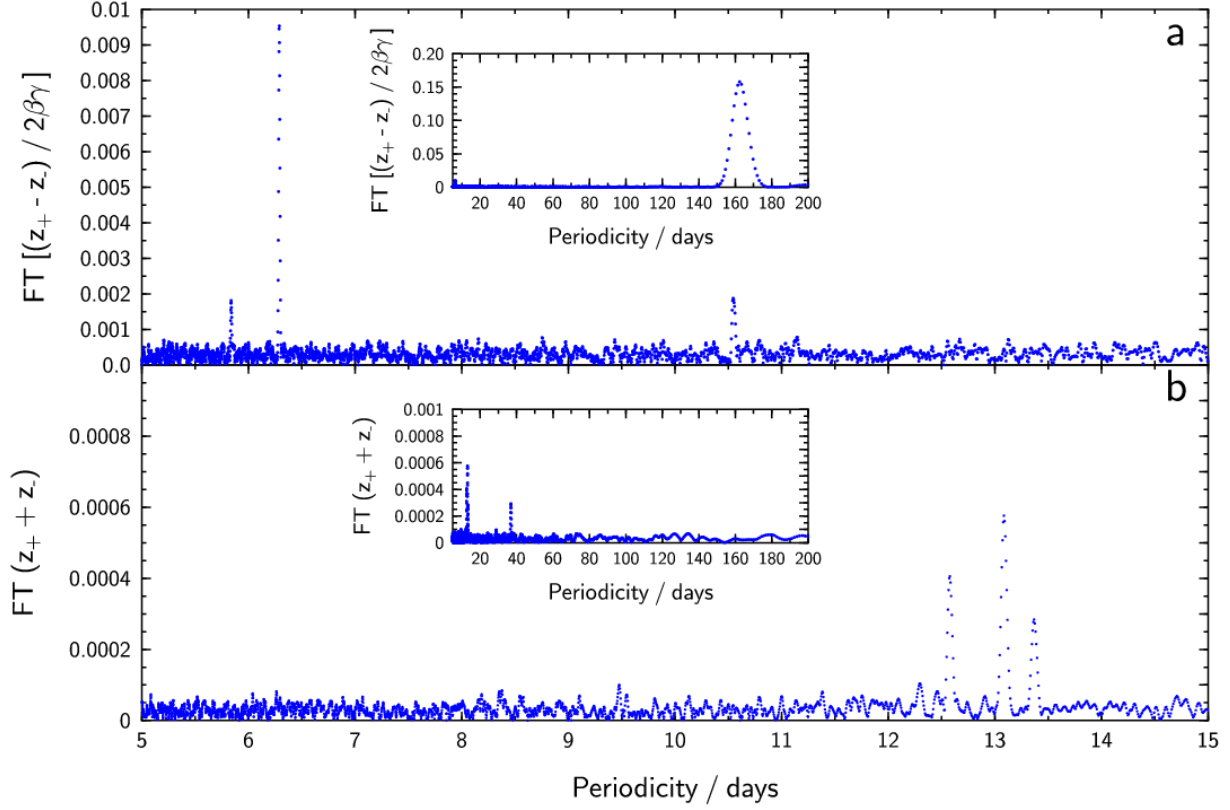


Fig. 2.— Fourier transform of data as described in §3. **(a)** The data transformed are the differences of all redshift pairs, divided by  $2\beta\gamma$  (see Eqn 3) which, if the jets are symmetric, should correspond to an expression only depending on the angular properties of the jet. The transform recovers periodicities at 5.8 and 6.3 days — the known locations of the nodding of the jet axis. **(b)** The data transformed are the sums of all redshift pairs which, if the jets are symmetric, should correspond to an expression only depending on the speed of the jet (see Eqn 2).

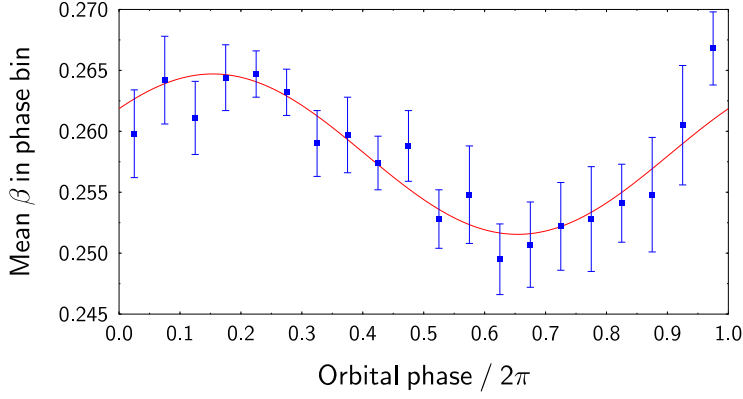


Fig. 3.— Speed data (Eqn 2) folded over the orbital period of 13.08 days showing a clear sinusoid, whose best fit parameters are: mean =  $0.2581 \pm 0.0005$ , amplitude =  $0.0066 \pm 0.0007$ , phase offset with respect to optical ephemeris phase origin =  $2.17 \pm 0.11$  rad. Note that although this phase origin is often referred to as inferior conjunction, asymmetric structure in the accretion disc means it is unlikely that the minimum in the optical light curve corresponds to alignment of the two stars along the line-of-sight, so a phase offset of  $\pi/2$  would not be expected even if the oscillations were due to SS 433’s own orbital motion.

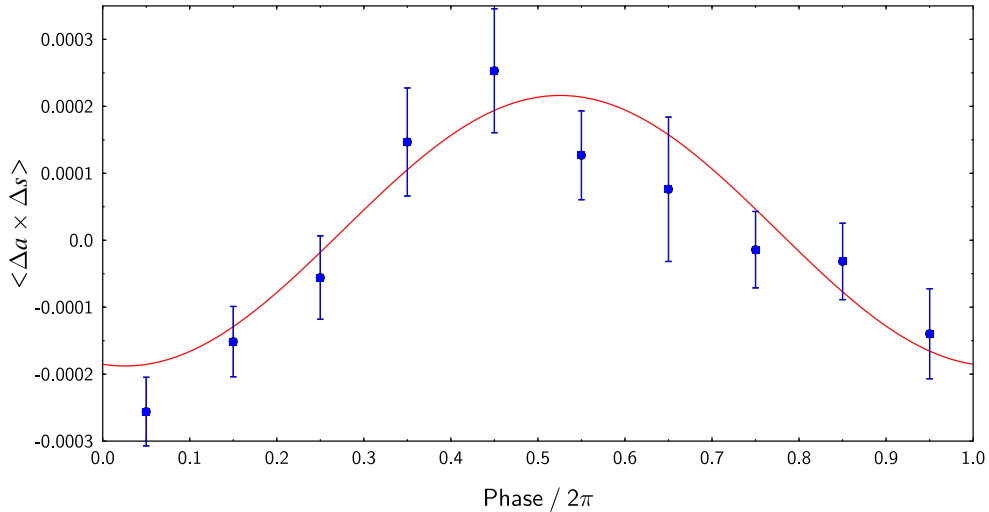


Fig. 4.— The mean value of  $\langle \Delta a \times \Delta s \rangle$  in given 162-day period phase bins, showing the best fit to Eqn 6. There are two free parameters in this fit, namely  $\langle \Delta \beta \Delta \theta \rangle$  and  $\langle \Delta \beta \Delta \phi \rangle$ .

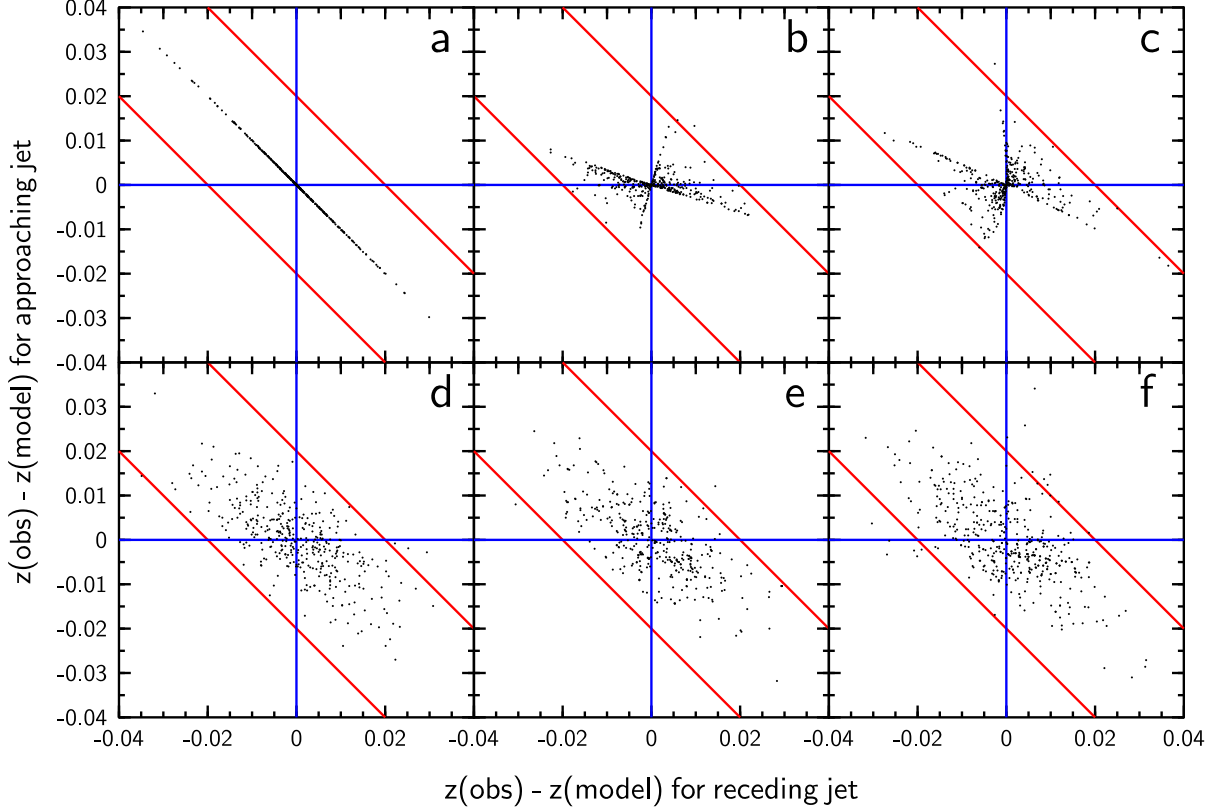


Fig. 5.— The effect on redshift residuals in each jet for different deviations from the kinematic model in  $\theta$ ,  $\beta$  and  $\phi$ , for each date on which there is a record in Collins’ dataset (to replicate the sampling function). **(a)** Variations only in  $\theta$ , drawn from a gaussian distribution whose half-width is 2.7 degrees. The form of this plot, namely points lying only on the  $y = -x$  line, is identical for variations only in  $\phi$ , or for variations in both  $\phi$  and  $\theta$ . **(b)** Speed-only variations (on a given day the velocity is drawn from a gaussian distribution with half-width 0.013 — Fig 1c). **(c)** Variations in speed *anti-correlated* with those in  $\theta$ : on a given synthesized observation date the same randomly-drawn number from a gaussian is scaled by 0.013 for the speed variation and by  $-2.7$  degrees for the  $\theta$  variation. **(d)** As (c), but the  $\theta$  variation is scaled by 0.6, and an un-correlated  $\theta$  variation of two-thirds the size of this is added, as is an un-correlated component in  $\phi$  drawn from a gaussian with half-width of 2.95 days. **(e)** As (d), but the duration of the velocity variations, and that of the correlated  $\theta$ -component, is drawn from a gaussian with a half-width of two days. **(f)** Actual residuals from Collins’ dataset.

### A. Conventions and phases

Comparison of various past analyses of optical data can be hindered by the different conventions used to describe the phase of the precession of SS 433's jets. There are three conventions we are aware of in the literature which are described in Table 2.

To evaluate the phase of the precession, in a given convention, on Julian day number  $JD$ , the following may be employed:

$$\phi_{(j)} = [JD - t_{0(k)}] \times \frac{2\pi}{P} + \psi_{(k \rightarrow j)} \quad (\text{A1})$$

where  $t_0$  is the phase origin in that same convention and  $P$  is the period of precession,  $j$  labels in which convention (A,B or C) the phase is being quoted, and  $k$  labels which if any of these conventions is being converted from.

To convert between conventions A and C,  $\psi_{(A \rightarrow C)} = \pi$  in Eqn A1. To convert from convention B to convention C,  $\psi_{(B \rightarrow C)} = \pi - \arccos(-\cot \theta \cot i)$  in Eqn A1. Note that this depends on the values of  $\theta$  and  $i$  a touch more than one might expect:  $\psi = 0.727\pi$  for  $\theta = 18^\circ$  and  $i = 78^\circ$  while  $\psi = 0.661\pi$  for  $\theta = 20^\circ$  and  $i = 80^\circ$ . For typical values of  $P$ , the difference between these two extreme values of  $\psi$  corresponds to a difference of 5 days.

The values of  $t_0$  (as modified Julian day) and  $P$  are quoted in the literature to be known to a few hundredths of a day; respectively:  $3561.75 \pm 0.42$  and  $162.677 \pm 0.074$  (Anderson, Margon, & Grandi 1983);  $3562.37 \pm 0.30$  and  $162.507 \pm 0.03$  (Margon & Anderson 1989);  $3563.23 \pm 0.11$  and  $162.375 \pm 0.011$  (Eikenberry et al 2001). It is clear from inspection of this list of numbers that (unsurprisingly)  $t_0$  and  $P$  are correlated. It is only if one or other of  $t_0$  and  $P$  could be determined independently that the uncertainty on the other could be quoted with this kind of accuracy. Consideration of these numbers, together with our own fitting of the same data leads us to believe that the period is known to 0.1 day. There have been over 57 precession periods since SS 433 was first discovered to have moving emission lines (Liebert et al. 1979; Margon et al 1979), so propagating this uncertainty from  $t_0$  to the present day gives a further uncertainty of  $> 5$  days over that identified in the preceding paragraph.

We believe that these two uncertainties are the true explanation of the claim of Stirling et al (2002) that the kinematic model was leading contemporaneous optical and radio observations of SS 433 in 1991/2 by 7 – 10 days. We know of no evidence that there was any step function in the mean phase of SS 433's behaviour at any point in the last 25 years.

Table 2. A summary of the conventions describing the phase of SS 433.

Label	Description	$\cos \psi$ (Eqn A1)	Used by
A	west jet maximally redshifted	+1	1
B	jets in plane of sky (most recently after maximum separation of moving lines)	$-\cot \theta \cot i$	2,3,4
C	east jet maximally redshifted	-1	5,6,7

References. — (1) Eikenberry et al (2001) figures, (2) Anderson, Margon, & Grandi (1983), (3) Eikenberry et al (2001) table 1, (4) Margon (1984), (5) Kemp et al. (1986), (6) Stirling et al (2002), (7) Vermeulen (1989)